ELSEVIER

Materials Chemistry and Physics 77 (2002) 632–638

MATERIALS CHEMISTRY AND PHYSICS

www.elsevier.com/locate/matchemphys

Role of an intermediate phase $(Ba,Sr)_2Ti_2O_5CO_3$ in doped $(Ba_{0.7}Sr_{0.3})TiO_3$ thin films

San-Yuan Chen [a], Hong-Wen Wang [b,*], Li-Chi Huang [a]

[a] *Department of Materials Science and Engineering, National Chiao-Tung University, Hsinchu 300, Taiwan, ROC*
[b] *Department of Chemistry, Chung-Yuan Christian University, 22 Pu-Ji, Chung-Li 320, Taiwan, ROC*

Received 10 July 2001; received in revised form 21 September 2001; accepted 19 November 2001

Abstract

$(Ba_{0.7}Sr_{0.3})TiO_3$ (BST) thin films doped with La, Nb, and Mg ions were prepared by metal-organic deposition method (MOD) on $Pt/Ti/SiO_2/Si$ substrates. An intermediate phase formed under an annealing temperature of 550–650 °C, and disappeared at higher temperatures during the formation of BST. The intermediate phase was analyzed by X-ray diffraction (XRD) analysis, transmission electron microscopy (TEM), Fourier transform-infrared spectroscopy (FT-IR) and Raman spectra and found to be an oxycarbonate with a chemical formula of $(Ba,Sr)_2Ti_2O_5CO_3$. The stability of this intermediate phase increased with the addition of dopants, irrespective of doping types. It is proposed that distortion of crystal structure, physical constraint in the two-dimensions and small grain size favor the existence of poor crystallized $(Ba,Sr)_2Ti_2O_5CO_3$.

Keywords: Intermediate phase; $(Ba,Sr)_2Ti_2O_5CO_3$; BST thin film; MOD

1. Introduction

Chemical solution deposition methods such as sol–gel deposition and metal-organic decomposition (MOD) method are widely used as a relative easy and flexible technique for thin film preparation [1–3]. $(Ba_{0.7}Sr_{0.3})TiO_3$ (BST) thin films have been intensively investigated for their great potentiality in high-density-gigabit DRAM applications [4]. Recently, during the preparation of BST thin films, Kasenkox et al. [5] and Liedtke et al. [6] have found an intermediate phase at $2\theta \cong 27^\circ$ and attributed this oxycarbonate phase as $Ba_2Ti_2O_5CO_3$. This oxycarbonate phase has been reported as an intermediate phase during the preparation of barium titanate ($BaTiO_3$) by different chemical solution methods [7–9]. However, the nature of this intermediate phase is not well-understood. Previous studies all show the same diffuse signals in their X-ray powder diffractograms and could not be identified to any known substance. Kumar et al. [7] assigned the X-ray powder diffractogram to be the $Ba_2Ti_2O_5CO_3$ phase, and the $BaTiO_3$ phase forms directly by the endothermic decomposition of this phase between 635 and 700 °C. A similar formula, $Sr_2Ti_2O_5CO_3$, for the intermediate phase, was also successfully identified by Leite et al. [10] during the preparation of $SrTiO_3$ by Pechini method. In the decomposition of barium titanium citrate, Hennings et al. [11] described the intermediate phase as a mixture of $BaCO_3$ and TiO_2 in finest distribution. From X-ray photoelectron spectroscopy results, Cho [12] concluded that intermediate phase is not a barium titanium oxycarbonate but hexagonal $BaTiO_3$ stabilized with Ti^{3+} ions. It seems that these intermediate phases function as a key component in the formation of $BaTiO_3/SrTiO_3$ phase derived from organic precursors. However, the oxycarbonate or the barium carbonate intermediate phase seems to behave differently in various BT-related bulk and thin film materials. In the present study, an attempt has been made to investigate the phase evolution of $Ba_2Ti_2O_5CO_3$ in BST thin film. The role of dopants in the stability of the intermediate phase and the formation of BST phase is also discussed.

2. Experimental procedure

The starting materials used for the study was barium acetate $Ba(CH_3COO)_2$, strontium acetate $Sr(CH_3COO)_2$, titanium *n*-butoxide $Ti(C_4H_9O)_4$, lanthanum acetate $La(CH_3COO)_2$, niobium ethoxide $Nb(OC_2H_5)_5$, magnesium methoxide $Mg(OCH_3)_2$. Glacial acetic acid (CH_3COOH) and 2-methoxyethanol ($C_3H_8O_2$) were used as solvents. The

* Corresponding author.
E-mail address: hongwen@cycu.edu.tw (H.-W. Wang).

0254-0584/02/$ – see front matter
PII: S0254-0584(02)00009-3

stock solutions of desired compositions were prepared by established MOD method. After dissolving barium acetate and strontium acetate to acetic acid completely, titanium *n*-butoxide was added to the mixture with constant stirring. The solution of La, Nb, and Mg were also added to the resulting BST solution in various molar concentrations. Finally, the 2-methoxyethanol was used to adjust the viscosity of the solution. The concentrations of dopants (La, Mg, and Nb) to BST solution were 1, 5, 10, and 15 mol%, respectively. To keep stoichiometry of ABO_3, the formula of present study were $((Ba_{0.7}Sr_{0.3})_{1-x}D_x)TiO_3$, for site A and $(Ba_{0.7}Sr_{0.3})(Ti_{1-x}D_x)O_3$ for site B, where D represents the dopants. It is generally assumed that La goes to A site as a donor, Mg to B site as an acceptor, and Nb also to B site as a donor. The stock solutions were filtered by 0.2 μm syringe filters before thin film deposition.

The filtered solutions were deposited on platinized Si wafer ($Pt/Ti/SiO_2/Si$) by two-step spin-coating (1000 rpm, 10 s, and 6000 rpm, 30 s). The wet coatings were pyrolyzed at 550–800 °C for 10 min. The deposition–pyrolyzing process was repeated in order to achieve the desired thickness. The final films were annealed at corresponding temperatures for 1 h. The phase development was investigated using X-ray diffraction analysis (XRD, Rigaku, Model D/MAX III.V) with a copper target, a speed of $1^\circ\,min^{-1}$ under 30 kV, 20 mA. The surface morphology and thickness of films were examined by field emission scanning electron microscopy (FESEM, Hitach S-4000). Grain size has been determined using transmission electron microscopy (TEM, JOEL-2000FX) images. The films were cross-sectioned, ion-milled, and observed under 200 kV. Selected area diffraction pattern (SADP) is utilized to identify its crystalline phase. Further examinations of the intermediate phase were done by FT-IR and Raman spectroscopy. The Fourier transform-infrared spectroscopy (FT-IR, Nicolet Model 460) was performed by grinding the specimen down to some 400 mesh powders, pressing the powders into a 12 mm diameter disk with 99 wt.% of KBr (Merck) and collecting the absorption data from 500–4000 cm^{-1}spectra in a resolution of 1 cm^{-1}. The Raman spectroscopic experiment (France, Modular X-Y DILOR Spectrometer) was done by lighting Ar ion laser ($\lambda = 519$ nm) on the specimen after focusing and collecting the Raman scattering data.

3. Results

3.1. Phase development

Fig. 1 shows the XRD patterns of pure BST films annealed at 550–800 °C for 1 h. At 550 °C, no peaks of crystalline phase were found. At 600 °C, a broad diffraction peak ranging at $2\theta = 26$–28° was clear. However, this intermediate phase disappeared at 650 °C and the crystalline BST phase showed-up. The BST crystalline phase becomes strong as the temperature increases to 800 °C. The similar intermediate phases were also found in the phase development of La-, Nb-, and Mg-doped BST films. Fig. 2(a–d) show the XRD patterns for La-doped BST films at various annealing temperatures. The intermediate phase were stable up to 650 °C when dopant concentration was below 10 mol%, and even stable at 700 °C for the 15 mol% La-doped sample. As a result, the formation of BST perovskite phase occurring at 650 °C in pure BST films was suppressed in the 15 mol% La-doped sample due to the stability of intermediate phase. The behavior of phase development for various Nb- and

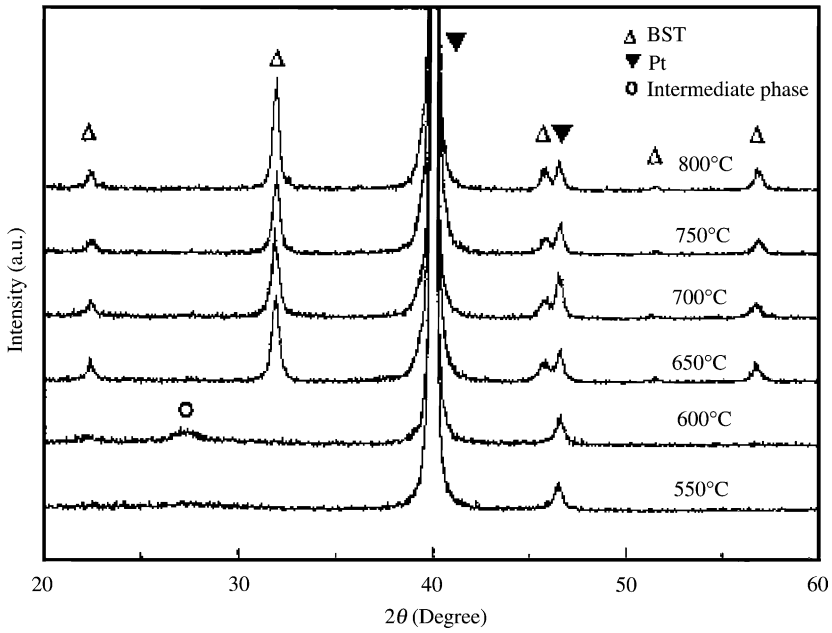

Fig. 1. XRD diffraction patterns for BST film annealed at 550–800 °C for 1 h.

Mg-doped BST films are very similar to those of La-doped samples. Their XRD patterns are very much the same as those of La-doped BST films and will not be shown. The intermediate phase was also stable at 650 °C and the formation of BST crystalline phase as well as the disappearance of this intermediate phase must be up to 700 °C. However, well and pure BST crystalline films for all doped samples can be always obtained by annealing at temperatures over 750 °C.

3.2. The intermediate phase

From the XRD patterns, the intermediate phase around $2\theta \cong 27^\circ$ could possibly be the reported oxycarbonate phase $Ba_2Ti_2O_5CO_3$. To confirm the existence of this phase, we further calcined the pure BST solution into powders at different temperatures for comparison. Both powders and thin films are further analyzed by FT-IR, Raman spectroscopy and TEM selected area diffraction pattern (SADP). Fig. 3 shows the XRD diffraction patterns for BST powders after calcinations at different temperatures. In addition to the intermediate phase observed at $2\theta \cong 27^\circ$ in the thin film specimens, there are another more evident intermediate phases at $2\theta \cong 24.1$ and 34.2°, especially for the BST powder calcined at 575 °C (Fig. 3(d)). From the reported literatures [13,14], it can be recognized that the intermediate phase at $2\theta \cong 24.1$ and 34.2° are barium carbonate $BaCO_3$.

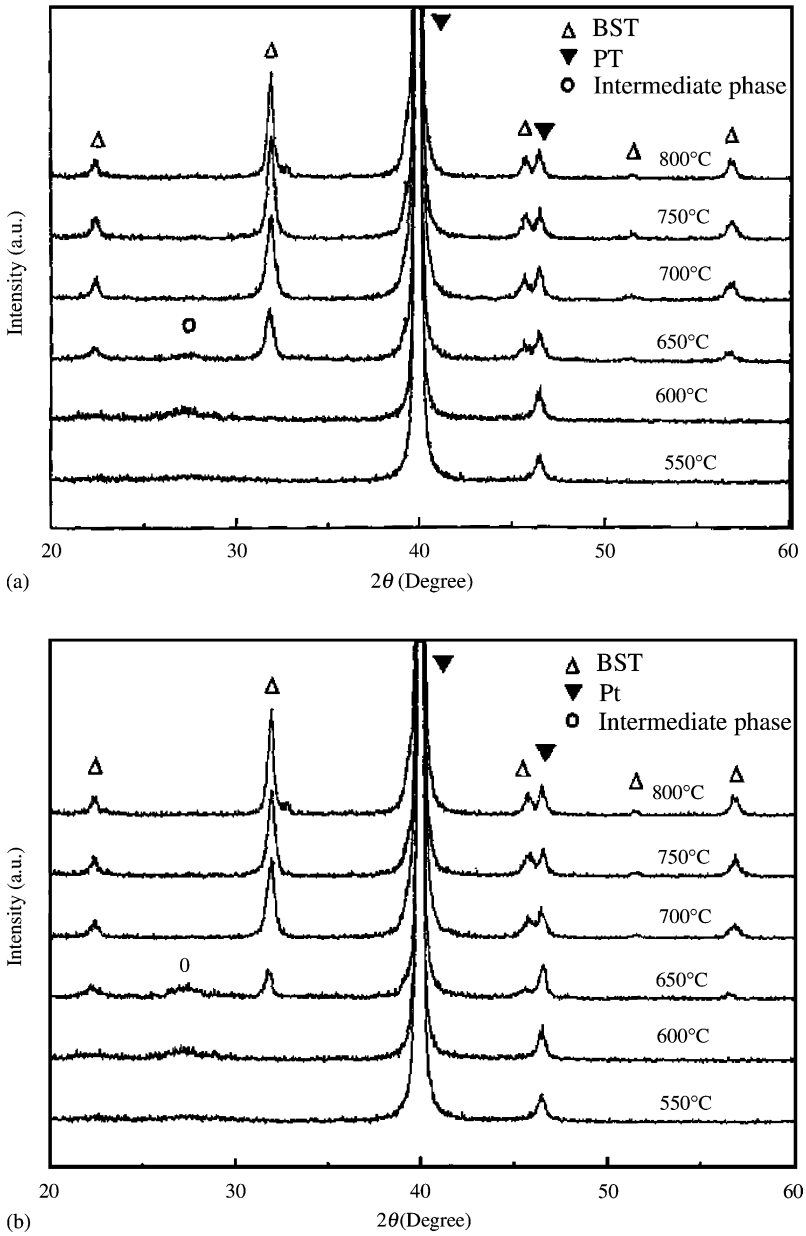

Fig. 2. XRD diffraction patterns for La-doped BST films annealed at various temperatures for 1 h. (a) La = 1 mol%, (b) La = 5 mol%, (c) La = 10 mol%, and (d) La = 15 mol%.

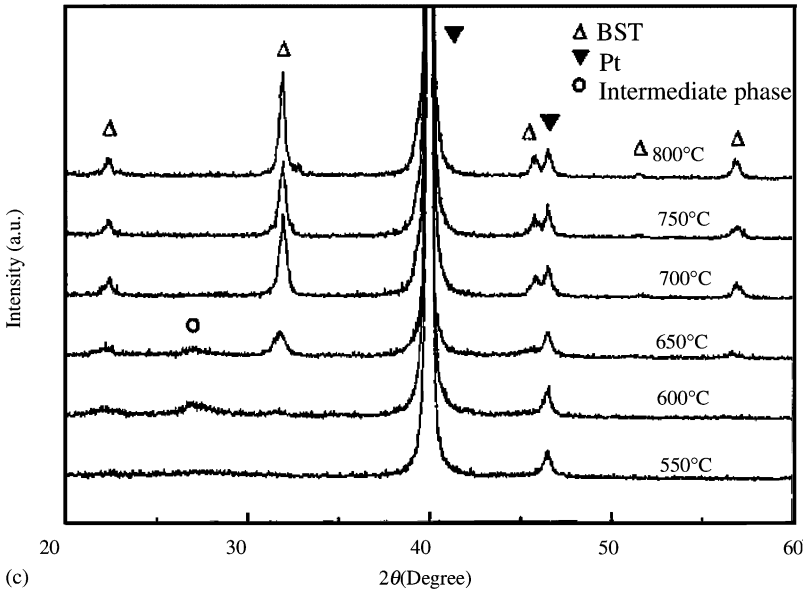

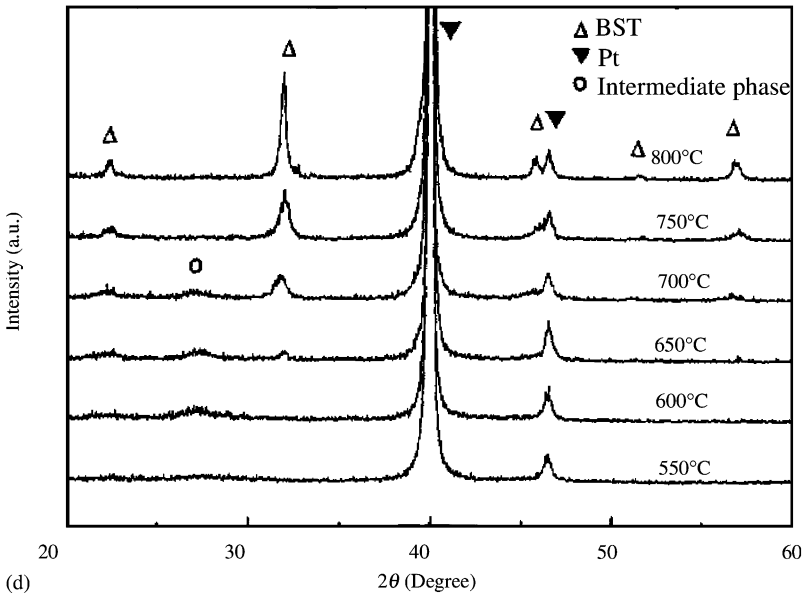

Fig. 2. (*Continued*).

Further examination by FT-IR on the ceramic powders revealed the existence of carbonate ions as shown in Fig. 4. The absorbance peaks [15] at wave number 1451, 1050 and 857 cm^{-1} belongs to CO_3^{-2}, while those [16] at 1090 and 880 cm^{-1} are caused by the vibration of C–O and C–C bonds. The Raman spectrums shown in Fig. 5 are obtained from the ceramic powders. As the calcinations temperatures go up to 700 and 800 °C, well crystalline phases are evident from the wave number 521 cm^{-1}. In the range of 500–575 °C, only a small peak at 1061 cm^{-1} is shown. This is attributed to the existence of CO_3^{-2}.

The TEM image and SADP in Fig. 6 provide a direct observation of the intermediate phase. The ring distance is correspondent to the $2\theta = 26.8^{\circ}$ diffraction data which was reported by Kumar et al. [7]. We, therefore, confirmed that the phase is $(Ba,Sr)_2Ti_2O_5CO_3$-related. According to Kasenkox et al. [5], it is more appropriate to state that the intermediate phase is $(Ba,Sr)_2Ti_2O_5CO_3$ rather than $Ba_2Ti_2O_5CO_3$, since the materials in present study is $(Ba,Sr)TiO_3$. A few brighter spots are clear in the diffraction rings, which may be resulting from several stronger crystalline units in the film. However, the amorphous diffuse ring pattern implies that the crystallanity of this intermediate phase is poor.

3.3. Microstructures

Fig. 7(a–d) show the microstructures of La-doped BST films annealed at 750 °C for 1 h. As the dopant concentra-

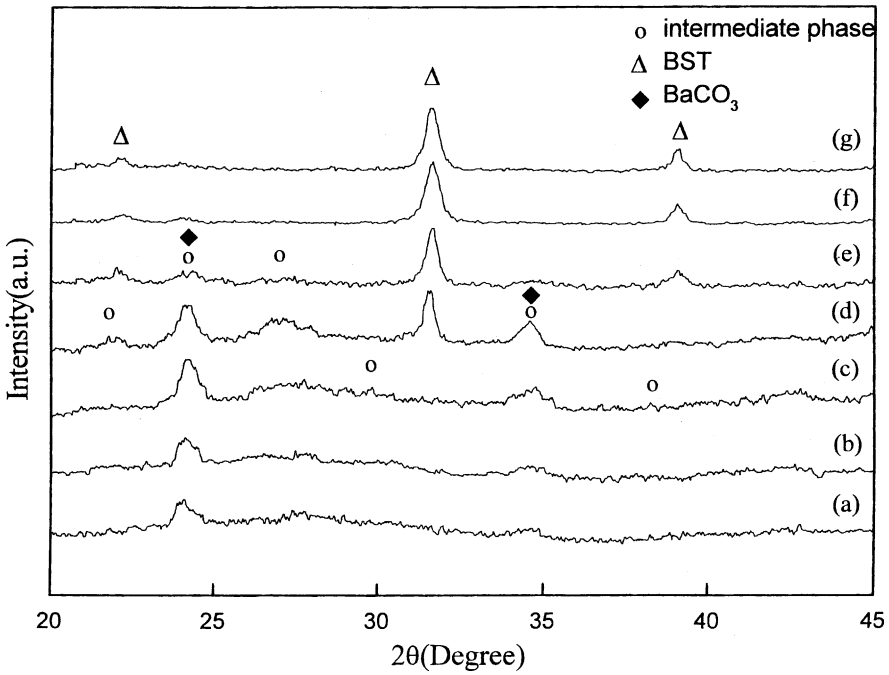

Fig. 3. XRD diffraction patterns for BST powders after calcinations at different temperatures. (a) 500 °C, (b) 525 °C, (c) 550 °C, (d) 575 °C, (e) 600 °C, (f) 700 °C, and (g) 800 °C.

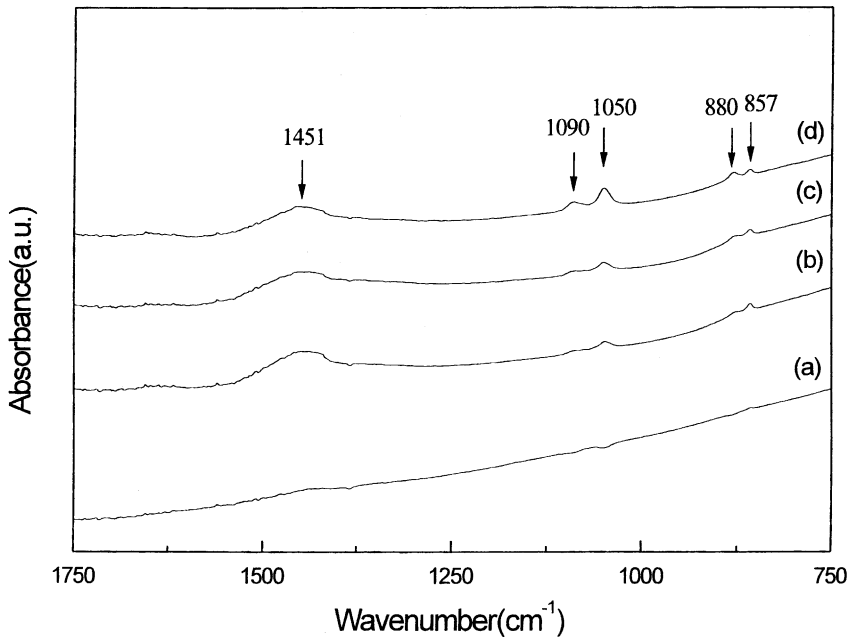

Fig. 4. FT-IR for BST powders after calcinations at (a) 500 °C/h, (b) 525 °C/0.5 h, (c) 525 °C/h, and (d) 550 °C/0.5 h.

tion increases, the grain size decreases. Similar grain size inhibition effect due to addition of dopants is also observed in Nb- and Mg-doped BST films. To estimate the grain size correctly, TEM images were used. Grain sizes of doped BST films annealed at 750 °C are summarized in Table 1. Grain size reduces to half when dopant concentration is up to 15 mol%.

Table 1
Grain size (unit: nm) of doped BST films annealed at 750 °C

	0 mol%	1 mol%	5 mol%	10 mol%	15 mol%
La	45.9	44.0	35.9	26.9	22.0
Nb	45.9	32.2	30.4	24.7	22.9
Mg	45.9	33.8	29.9	28.3	26.5

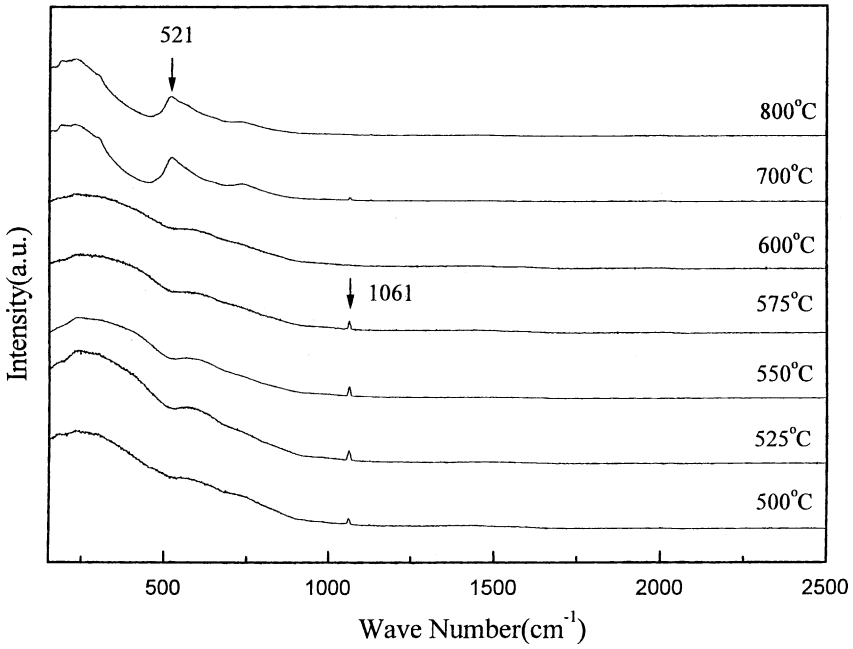

Fig. 5. Raman spectra for BST powders after calcinations at various temperatures.

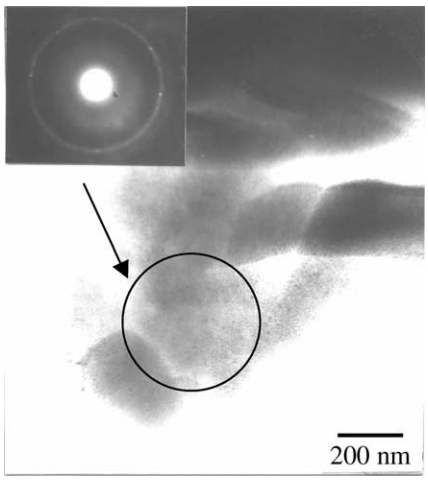

Fig. 6. TEM image and SADP for the intermediate phase of BST films. The ring distance is correspondent to the $2\theta = 26.8^\circ$ diffraction data.

4. Discussion

From the XRD results of pure BST thin films, the $(Ba,Sr)_2Ti_2O_5CO_3$ phase was identified starting at 600 °C and disappeared at 650 °C. The formation of BST crystalline phase is evident at 650 °C in pure BST film. However, the addition of dopants not only stablized $(Ba,Sr)_2Ti_2O_5CO_3$ at 650 °C but also suppressed the formation of BST crystalline phase. The formation of BST crystalline phase must go up to 700 °C due to the addition of dopants. The existence of $(Ba,Sr)_2Ti_2O_5CO_3$ can even be observed at 700 °C in 15 mol% La-doped sample. In other words, the addition of dopants extends the stability temperature domain of $(Ba,Sr)_2Ti_2O_5CO_3$ phase. The formation of BST phase is always accompanied by the disappearance of this oxycarbonate phase. Since the stability of the oxycarbonate phase has been slightly increased at 650 °C in doped films, the formation of BST phase was slightly postponed to higher temperature (700 °C) in these samples.

In the ceramic powder derived from same chemical solutions, the intermediate phases were identified as $BaCO_3$ (major), and $(Ba,Sr)_2Ti_2O_5CO_3$ (minor). From the literatures and our previous experiences, it is often to observe $BaCO_3$ phase in the $BaTiO_3$ or BST ceramic powders as the intermediate phase. However, it is interesting to note that $BaCO_3$ was not found as an intermediate phase in thin films; that is, Ti ions seem more likely to stay with Ba ions in the case of thin films and form the $(Ba,Sr)_2Ti_2O_5CO_3$ phase. An important difference of this study from other works is that the dopant concentration is as high as 15 mol% and yet the materials were still a single perovskite crystalline phase. It is understandable that the dopants participate in the perovskite structure as it forms a single solid solution. The deviation from normal "order" perovskite BST crystal structure is likely to be increased by the addition of alien ions. The distortion of these doped BST crystal structures is high as compared to that of pure BST crystal structure.

It seems that the distortion of perovskite structure, the physical constraint in two-dimensions and small grain are three factors to favor the existence of poor crystalline $(Ba,Sr)_2Ti_2O_5CO_3$ phase. The addition of 15 mol% dopants decreases the grain size up to 50% in doped samples. Additionally, the crystal distortion and physical constraint are the highest in these samples. This agrees with the trend of increasing dopant concentration on the increasing stability

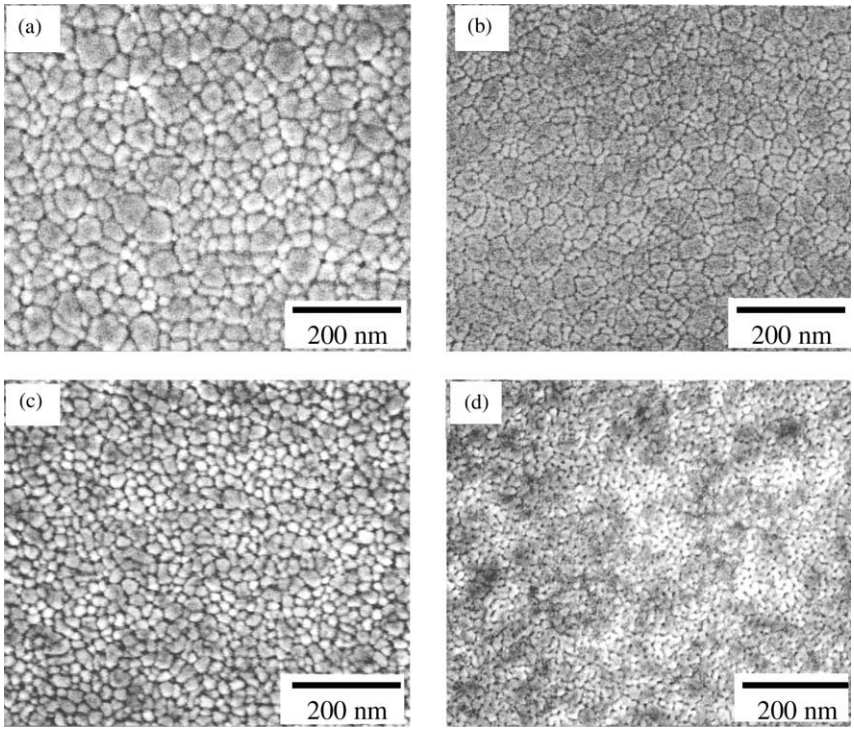

Fig. 7. It shows the microstructures of La-doped BST films annealed at 750 °C for 1 h. (a) La = 1 mol%, (b) La = 5 mol%, (c) La = 10 mol%, and (d) La = 15 mol%.

of $(Ba,Sr)_2Ti_2O_5CO_3$. In a study of barium titanate [17], it is also demonstrated that the tetragonality of perovskite phase has been suppressed into a cubic phase due to nanometer crystalline size. In such nanometer size and highly distorted structure as well as two-dimensional limitation space, the crystalline phase $BaCO_3$ and BST did not favor but the poor crystallized $(Ba,Sr)_2Ti_2O_5CO_3$ phase did.

5. Conclusion

The effect of dopants such as La, Nb and Mg on the phase formation and microstructure of BST thin films are studied by metal-organic deposition method. An intermediate phase $(Ba,Sr)_2Ti_2O_5CO_3$ during the development of crystalline BST thin films is confirmed. The distortion of structure and decreased grain size due to the addition of dopants extend the stability domain of $(Ba,Sr)_2Ti_2O_5CO_3$ intermediate phase and thus postponed the formation of crystalline BST phase. The intermediate phase is completely disappeared at 750 °C and well crystalline BST films result.

References

[1] D.M. Tahan, A. Safari, L.C. Klein, J. Am. Ceram. Soc. 6 (1996) 1593.
[2] P. Jana, R.K. Pandey, Intergr. Ferroelec. 17 (1997) 153.
[3] D.A. Neumayer, P.R. Duncombe, R.B. Laibowitz, A. Grill, Intergr. Ferroelec. 18 (1997) 297.
[4] P.Y. Lesaicherre, H. Yamaguchi, Y. Miyasaka, H. Watanabe, H. Ono, M. Yoshida, Intergr. Ferroelec. 8 (1995) 201.
[5] U. Kasenkox, S. Hoffmann, R. Waser, J. Sol–Gel Sci. Tech. 12 (1998) 67–79.
[6] R. Liedtke, S. Hoffmann, R. Waser, J. Am. Ceram. Soc. 2 (2000) 436.
[7] S. Kumar, G.I. Messing, W.B. White, J. Am. Ceram. Soc. 3 (1993) 617.
[8] S. Gablenz, H.P. Abicht, E. Pippel, O. Lichtenberger, J. Woltersdorf, J. Eur. Ceram. Soc. 20 (2000) 1053.
[9] D. Hennings, G. Rosenstein, S. Schreinemacher, J. Eur. Ceram. Soc. 8 (1991) 107.
[10] E.R. Leite, C.M.G. Sousa, E. Longo, J.A. Varela, Ceram. Int. 21 (1995) 143.
[11] D. Hennings, W. Mayr, J. Solid State Chem. 26 (1978) 329.
[12] W.S. Cho, J. Phys. Chem. Solids 59 (1998) 659.
[13] M.del C.B. Lopez, G. Fourlaris, B. Rand, F.L. Riley, J. Am. Ceram. Soc. 7 (1999) 1777.
[14] M. Stockenhuber, H. Mayer, J.A. Lercher, J. Am. Ceram. Soc. 76 (1993) 1185.
[15] J.D. Tsai, Ph.D. thesis, National Cheng-Kung University, Taiwan, ROC, 1999.
[16] K. Nakamoto, Infrared and Raman Spectra of Inorganic and Coordination Compounds, 4th Edition, Wiley New York, USA, 1986, p. 476.
[17] K. Uchino, E. Sadanaga, T. Hirose, J. Am. Ceram. Soc. 8 (1989) 1555.